# Characterization of laser diodes under short-pulsed conditions with high pulse energies

Tobias Koenning*, Evan Hale, David Irwin, Kim Alegria, Steve Patterson
DILAS Diode Laser Inc., 9070 South Rita Road, Suite 1500, Tucson AZ 85747

## ABSTRACT

New applications require diode lasers to be driven with short pulses in the sub-micro second range. The goal is to minimize both the cost and size of the diode laser module by minimizing the number of laser bars required while maintaining the lifetime that is desired for the application. Products demanded by the market using such short pulses range from QCW stacks to fiber coupled modules. While many short pulsed applications use high fill factor bars, these bars are not suited for high brightness applications or coupling into small fiber cores. The focus of this work is the analysis of CW diode designs commonly used for high brightness fiber coupled modules under short pulsed conditions.

Three key parameters need to be known in order to design a diode laser module that is suited for high peak powers. First is the damage threshold of the facet. The damage threshold determines the maximum power level at which the laser can be operated safely, considering a proper safety margin dependent on application. The damage threshold is a function of the input pulse width and amplitude. The second parameter which is influenced by the drive current is the slow axis divergence of the diode laser. Knowledge of this parameter is critical when designing the system optics. The third parameter is the effective emitter size which may increase with operating current. An increase in emitter size will lead to larger divergences after collimating optics for a given focal length lens and may result in a larger spot when coupling into an optical fiber. All these parameters have to be considered when designing a new product.

Presented here is a study on these three critical parameters as a function of operating conditions. Results for different diode designs will be presented. The data presented includes damage thresholds, as well as near field and far field data at various operating currents. A design study for fiber coupled modules with high pulse energies based on the test results will be shown for various wavelengths.

**Keywords:** High power diode laser, fiber coupling, peak power, pulsed mode, damage threshold, industrial, defense

## 1. INTRODUCTION AND APPLICATIONS

Low cost drivers that permit sub-micro-second pulses at varying duty cycles, up to DC, have enabled new technologies in military and medical applications such as range finders, time resolved fluorescence microscopy and laser ignition. For many pulsed applications laser bars with high fill-factors are used in order to keep the facet intensity and current density low allowing very high peak power (relative to CW ratings). However, these bars suffer from low brightness and are not suitable for coupling into small fiber cores. High brightness and the ability to use optical fibers to guide the laser radiation are beneficial for many applications.

Much of the published reliability data is for high fill-factor bars [1]. However, there is little data available on the operation of low fill-factor bars under short pulsed, high current operation. Due to the lower fill-factor, both the current density and facet optical field intensity are higher at the same output power when compared to high fill-factor bars. Operating limits are often determined by damage thresholds in CW mode of operation. Under short pulsed conditions in the sub-micro-second range and low duty cycles self-heating is diminished and much higher power levels can be achieved [2].

While optical parameters such as exact emitter size and slow axis divergence may not be very critical for some low brightness applications, both have an immediate impact on the ability to couple into small fiber cores. In general, the slow axis divergence of a laser bar increases with operating power. This is particularly true of gain-guided devices. The

* t.koenning@dilas-inc.com; phone +1 (520) 282 5986; fax +1 (520) 232 3499; www.dilas.com

effective emitter size may also increase due to current spreading at higher current densities. Most low fill-factor bars have been properly qualified for CW mode of operation but the effects on emitter size and slow axis divergence when operating at high peak current but low duty cycle is not readily available in the published literature.

In order to design high brightness fiber coupled modules these parameters need to be known. The beam parameter product of the laser bar at the specified operating point determines the limit on the number of laser bars that can be coupled into a given fiber size effectively. If slow axis divergence or emitter size grows significantly at high peak currents, this has to be considered when designing the optical layout of the module and may set a limit on the total number of laser bars that may be used to achieve the specific power. On the other hand, it may be possible to reduce the number of laser bars required to achieve a given peak power or pulse energy if the peak operating current can be increased compared to the CW limit of the chip without damaging the laser bar or diminishing the diode's brightness.

While many efforts have been undertaken to improve both the crystal structure and the facet coating, COD (catastrophic optical damage) or COMD (catastrophic optical mirror damage) are still the main limitations to the maximum achievable output power from a laser bar. Once limitations set by the onset of catastrophic damage are remedied, other effects such as spectral and spatial hole-burning, carrier leakage, and carrier heating must be considered in the limits set on the achievable output power [2].

# 2. EXPERIMENTS

## 2.1 Methodology

All devices under test are standard bars qualified to operate CW, with 19 emitters and a 500µm pitch. Both 100µm nominal stripe (20% fill-factor) and 150µm nominal stripe (30% fill-factor) bars have been tested. The material covers center wavelengths of 790nm, 808nm, and 976nm. Bars are indium mounted onto passively cooled copper heat sinks (comparable to the industry standard CS-type submount). None of the bars has been treated with special facet passivation techniques to increase the COD threshold.

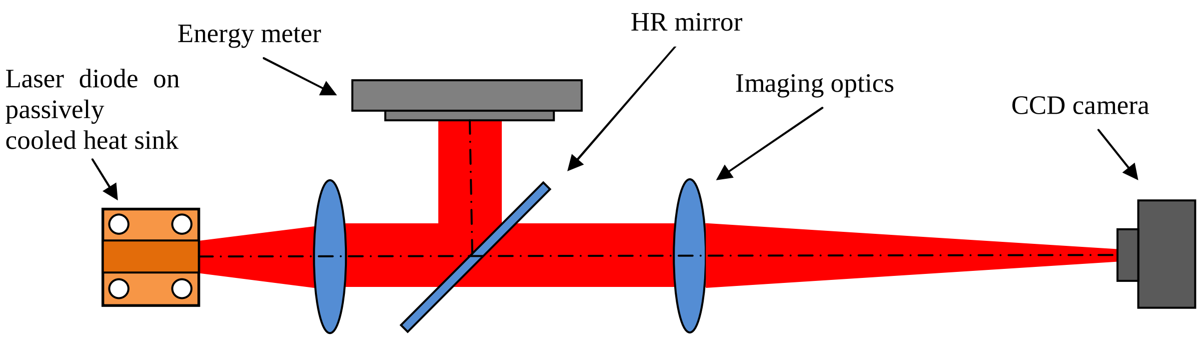


**Figure 1:** Top-down schematic of test setup.

As shown in Figure 1, the device under test is mounted to a base plate using mechanical reference edges to ensure good repeatability. The base plate is at room temperature (22ºC) and no active cooling is used. It is assumed that the unexcited active region temperature is also at room temperature. In a first series of tests the damage threshold and near field characteristics are determined. A high-current pulse-driver from Omnipulse (model PLDD-300-25-60) is used for all tests. A 45-degree mirror is used to direct the majority of the power to a Gentec energy meter (QE25SP-S-MT) to measure the pulse energy. This mirror also acts as an attenuator for the portion of the beam passing towards the CCD camera. An optical setup is used to image one emitter onto a CCD camera (Foculus FO323TB). A magnification of 75 is used in fast axis direction and a magnification of 15 in the slow axis direction. Using a long exposure time on the camera (about 1 second), a single shot is fired from the current driver without active synchronization between current driver and camera while the shutter is open. A high-pass spectral filter is used to block any visible light and ensures that a high signal-to-noise ratio is maintained.

Starting at a peak current of 50A, which is below the maximum rated CW current for all devices under test, the current is increased in increments of 10A. Pulse-to-pulse variations may be caused by both the current driver and the energy meter.

In order to minimize any such effect on the measurement, 10 shots each are fired at each current level at a repetition rate of 3Hz. The pulse energies of all 10 pulses are averaged. The typical standard deviation varies between three and five percent of the average pulse energy. The current pulse shape is monitored using the analog current monitor signal of the Omnipulse driver (Figure 2a). An InGaAs photodiode captures stray light from the energy meter. Both signals are captured using a TDS1001B oscilloscope. Similar to the methodology described by Olecki [3], a reference measurement at low current is taken after each high current test. A reference current of 50A is used and 10 pulses are fired after each high current increment to ensure that the laser bar has not been damaged. The operating current is increased until damage to the laser bar is indicated by reduced power of the reference pulses and the output power starts to decrease with increasing peak current (‘roll-over’). Sample test data is shown in Figure 2b. In addition to the 10 shots used for the power measurement, a single shot is fired at each current level to capture a near-field image of one emitter.

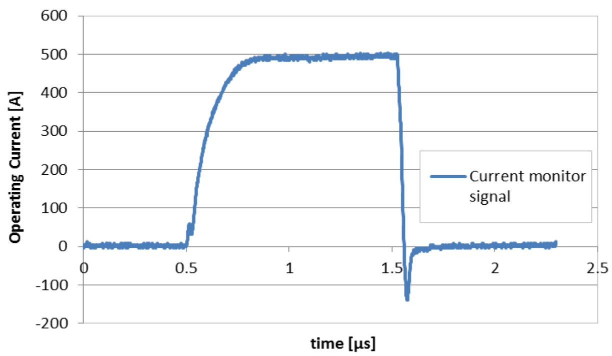


**Figure 2a:** 1µs pulse at 500A peak. Signal measured from current monitor of driver with laser diode connected. The negative swing at the end of the pulse is believed to be an artifact of the measurement.

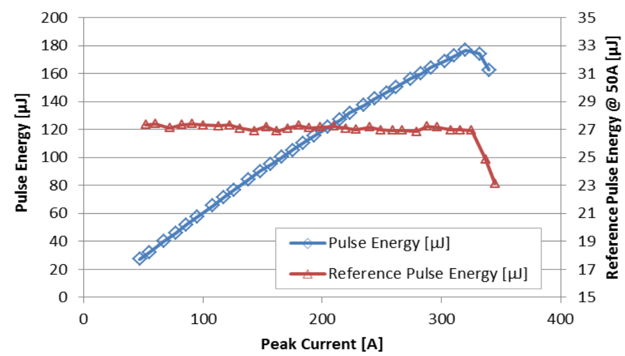


**Figure 2b:** S/N 117953 (808nm, 20% FF) tested at 0.6µs pulse duration.

The slow axis divergence is measured using a separate optical setup and with diodes that have not undergone the destructive damage threshold test. Again an exposure time of 1 second is used to limit synchronization problems between the current driver and the camera. A single shot is fired at each current level starting at 50A. The current is increased in 10A steps up to the damage threshold determined during the first test.

After damage has been detected by the reference pulse measurement described above, devices are inspected for signs of COD under the microscope.

## 2.2 Results

Figure 3 shows a summary of all damage threshold tests that have been conducted. Each datapoint shows the peak current achieved before the reference pulses indicated a significant decrease in pulse energy. Typically this point will coincide with a change in slope for the L-I curve. On some diodes the L-I curve rolls over immediately after the first damage occurs. The L-I curves taken from other diodes continue to gain in output power but with a reduced slope. This behavior can be explained by the different damage thresholds between single emitters on the same bar. Sometimes COD will occur in a tight current range for all emitters, sometimes one emitter shows an early failure while others continue to higher peak power. For the purpose of this test the first significant catastrophic event has been used to determine the failure point of the entire laser bar.

As stated by Eliseev [4] the damage threshold in the nanosecond range was identified as inversely proportional to the square root of the pulse width, shown as square root law in Figure 3. Kappeler [5] further states that for pulse widths greater than 1µs the damage threshold approaches the steady state value for the particular diode design and mounting scheme.

While the accumulated test data shown is not sufficient for a high confidence level statistical fitfunction for each chip material, the data nevertheless follows a fit that is proportional to the square root law and datapoints for each chip material align to a material specific inverse square root function. At 976nm, the current driver reached its limit of 500A peak current prior to any damage to the chip material for pulse width of 1µs and 2µs. Both datapoints have been marked with a red arrow pointing upwards in Figure 3 indicating that the actual damage threshold higher than the datapoints shown.

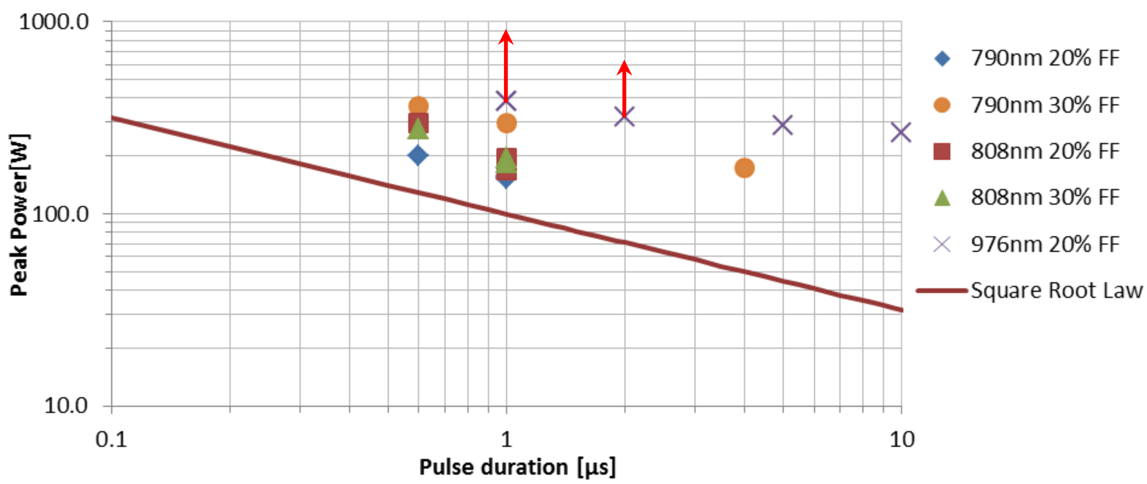


**Figure 3:** COD level for different chip materials at various pulse durations. Solid line represents 'square root law'. Red arrows indicate data were the maximum available drive current of 500A was reached before COD occurred.

To confirm that the failure mechanism observed in these tests is caused by COD, all diodes are visually inspected under the microscope at high magnification. All bars show signs of COD on one or multiple emitters. Figure 4 shows two representative images of COD. Each picture shows the area of one emitter at high magnification. As both pictures show, COD occurs in a random pattern in multiple locations across the width of the emitter. A more detailed explanation of the events that take place in COD is given by Tomm describing COD as a themal runaway process which starts with an elevated temperature at the facet or somewhere in the bulk of the semiconductor [6]. Once the process starts, surface recombination and surface current lead to futher heating of the facet while re-absorption of light due to the thermally diminshed band gap energy lead to a thermal runaway process inside the diode cavity.

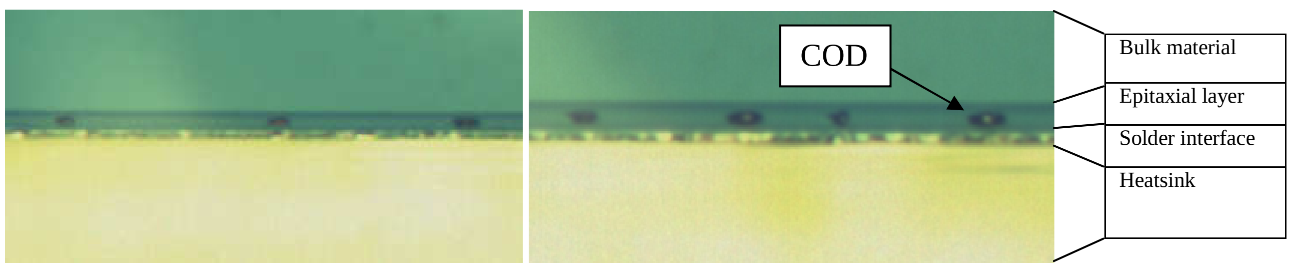


**Figure 4:** Image of front facet showing COMD (catastrophic optical mirror damage).

Figure 5a shows one near field image as it was acquired during the test. Similar images have been captured in increments of 10A for all chip materials up to the damage threshold. To minimize any influence of camera noise on the measurement, the beam width in the slow axis direction is calculated using the FWHM definition rather than an enclosed power (power in a bucket) definition.

Figure 5b shows a sample far field image. Similar to the near field, far field images have been acquired in 10A increments for all chip materials. Due to the reduced edge steepness of the profiles in the far field, a $1/e^2$ definition has been used to calculate the beam width as opposed to the FWHM definition used for the near field images.

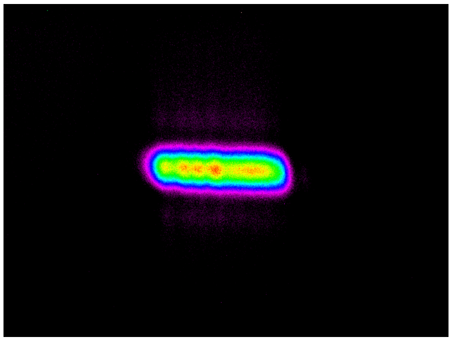

**Figure 5a:** Near field image showing 100um emitter.

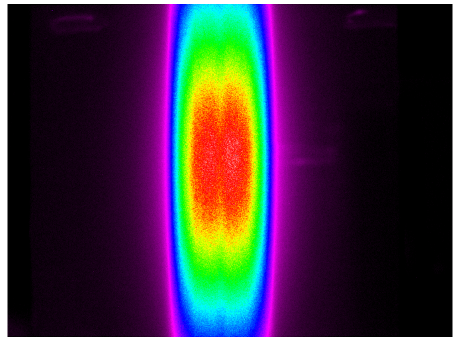

**Figure 5b:** Far field image ( 10 degrees slow axis divergence).

The results of the near field measurements are shown in Figure 6. At 976nm two bars have been tested at 1µs pulse duration and one bar has been tested at 10µs pulse duration. No significant increase of emitter size is observed with increased peak current. However, an increase of about 5µm in emitter width occurs when increasing the pulse duration from 1µs to 10µs.

Four diodes have been tested at 808nm. Two diodes had a nominal emitter width of 100µm (20% fill factor) and two diodes had a nominal emitter width of 150µm (30% fill factor). All four diodes show an increase in emitter size with increasing peak current on the order of 5%. All tests are performed at 1µs pulse duration.

At 790nm two diodes with 100µm emitter size (20% fill factor) have been tested at 1µs pulse duration. Both diodes show an increase in emitter size of about 3µm per 100A increase in peak current.

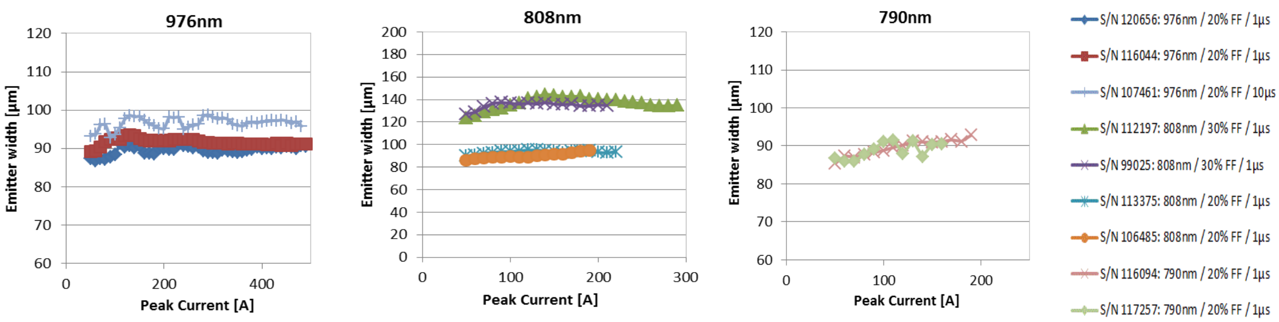


**Figure 6:** Emitter width (FWHM) measurements for different chip materials over peak current. Beam width measured with CDD camera.

Figure 7a shows divergence data for 976nm bars (20% FF) at 1µs and 10µs pulse duration. A steady increase with operating current can be seen. The slope is significantly higher at 10µs pulse duration compared to 1µs pulse duration. The slow axis divergence approaches 20 degrees ($FW1/e^2$) at 300A and 10µs pulse duration. At 1µs pulse duration the slow axis divergence is 17 degrees at 500A peak current.

Figure 7b shows similar results for 808nm and 790nm chip material. Due to the lower damage threshold determined in earlier tests, the divergence has only been measured up to 150A peak current. All tests at these wavelengths have been performed at 1µs pulse duration. The divergence at 150A peak current varies between 9.8 degrees and 10.2 degrees ($FW1/e^2$).

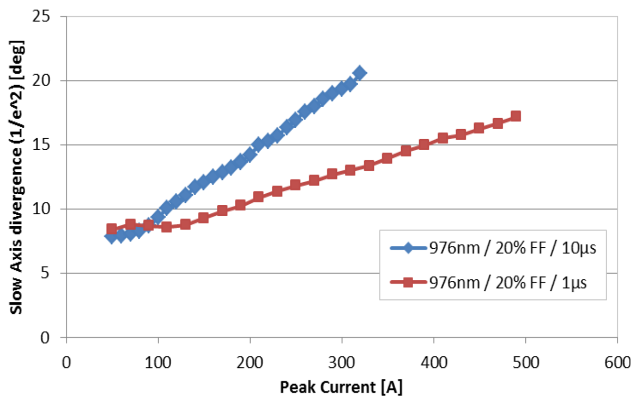


**Figure 7a:** Divergence of 976nm chip material plotted over peak current at 1µs and 10µs pulse duration.

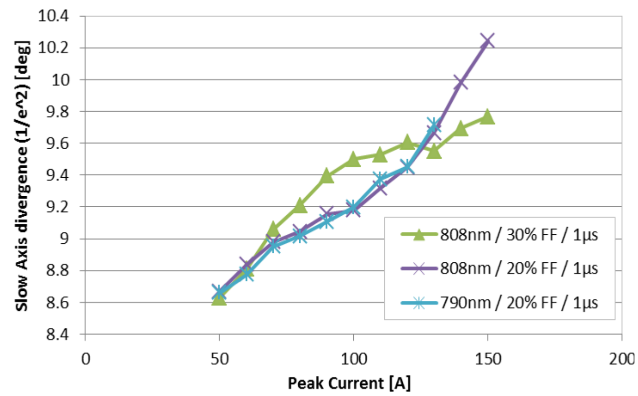


**Figure 7b:** Divergence of 808nm and 790nm chip material at 1µs pulse duration.

## 3. DISCUSSION

Based on the results shown above, diode laser bars can be operated at higher peak current with shorter pulse duration than their CW counterparts. Data supports the 'square root law' and coefficients for a fit function can be derived for each chip material. While decreasing emitter sizes generally lower the maximum peak power, an inhomogeneous intensity distribution on the front facet can lead to localized heating and lower the damage threshold further. Figure 5a shows such an intensity profile. The distribution is not only affected by effects inside the laser cavity, but also depends on external feedback, which can be caused by reflections from external optical surfaces (e.g. lenses).

The key finding of the tests shown here is that, for all materials tested, the emitter size only increases by a small margin; even at high peak current. On the other hand the divergence continues to grow in a mostly linear way with increasing peak current. Slow axis divergences in excess of 20 degrees (FW1/$e^2$) have been observed at 300A and 10µs pulse duration. Even at 1µs pulse duration the divergence goes up to 17 degrees at 500A. Typical CW divergence is about 7 degrees for this chip material at 60W optical power which matches the short pulse divergence. Multiple effects can cause the increase in slow axis divergence. Possible causes are stronger current spreading, higher temperature gradients between the center and the edges of the emitter [7], and gain induced index depression. Stronger current spreading can be neglected as a cause here because it would also be eminent in the near field in form of significantly increased emitter size. The increase in divergence impacts the beam parameter product (BPP) of the diode and directly affects the maximum achievable output power for fiber coupled modules with a given fiber diameter and NA (BPP).

In order to estimate the maximum achievable output power from a fiber coupled module, some assumptions are made. All calculations shown here are based on a commonly used optical setup for fiber coupling of diode laser bars. It is based on a micro-optical lens array which rotates each emitter by 90 degrees. Consequently all 19 emitters of each bar are stacked in fast axis direction with a pitch of 500um. In the slow axis direction only one emitter width remains and can be collimated using a single cylindrical lens. Due to factors like bar curvature ('smile') and imperfections of lenses and the mounting process it is assumed that the BPP in fast axis direction for all chip materials at all operating currents is 17.5 mm*mrad (half angle * beam radius). Furthermore, the nominal emitter size is used for all calculations because the increase in emitter size observed in earlier tests was low. According to Wang [8] the fiber coupling criterion for diode lasers is based on the sum of the BPPs in both orthogonal directions (fast and slow axis). If the sum of the BPPs is smaller than the fiber core radius times the NA, the radiation can be coupled efficiently into the fiber. If the sum of the BPPs is significantly smaller than the beam quality required for fiber coupling, multiple bars can be stacked on top of each other. The BPP ratio shown in both tables is the fiber BPP divided by the sum of both orthogonal BPPs of the laser bar.

Table 1 and Table 2 show examples for the maximum achievable peak power from 400µm and 200µm fiber cores respectively, both with a NA of 0.22. All numbers shown are for pulse durations of 1µs. The numbers are based on the COD power and have to be reduced in order to operate safely below the COD threshold. A nominal multiplier of 0.85 has been applied to account for losses through the optical train. Similar calculations can be performed for other pulse durations. By use of polarization beam combining the amount of bars per module can be doubled. This almost doubles the maximum achievable output power from the fiber coupled module. Currently released CW fiber coupled modules at Dilas are rated at 50W per bar at 808nm and 976nm and 40W per bar at 790nm for a 400µm core fiber. For 200µm fiber core diameter the rated power is 40W for 808nm and 976nm and 32W for 790nm.

| Wavelength | Emitter size [um] | SA divergence [mrad] | BPP ratio | Peak power per bar [W] | # of bars | Peak power per module [W] |
|---|---|---|---|---|---|---|
| 790 | 100 | 171.0 | 2.02 | 150 | 2 | 255 |
| 790 | 150 | 174.5 | 1.83 | 290 | 1 | 246.5 |
| 808 | 100 | 178.0 | 2.00 | 180 | 2 | 306 |
| 808 | 150 | 178.0 | 1.82 | 180 | 1 | 153 |
| 976 | 100 | 296.7 | 1.77 | 390 | 1 | 331.5[1] |

**Table 1**: Peak power achievable from 400um fiber core (0.22NA)

| Wavelength | Emitter size [um] | SA divergence [mrad] | Max. # of bars | Peak power per bar [W] | # of bars | Peak power per module [W] |
|---|---|---|---|---|---|---|
| 790 | 100 | 171.0 | 1.01 | 150 | 1 | 255 |
| 790 | 150 | 174.5 | 0.91 | 290 | 1[2] | 246.5 |
| 808 | 100 | 178.0 | 1.00 | 180 | 1 | 306 |
| 808 | 150 | 178.0 | 0.91 | 180 | 1[2] | 153 |
| 976 | 100 | 296.7 | 0.88 | 390 | 1[2] | 331.5[1] |

**Table 2**: Peak power achievable from 200um fiber core (0.22NA)

## 4. SUMMARY

High power diode laser bars at wavelengths of 790nm, 808nm, and 976nm have been tested at various pulse durations ranging from 0.6µs to 10µs. Devices with both nominal 100µm emitter width (20% fill factor) and nominal 150µm emitter width (30% fill factor) have been tested. All devices under test were standard bars intended for CW use and no special facet passivation has been used. In addition to damage thresholds, the optical characteristics have been analyzed at short pulse durations between 0.6µs and 10µs and high pulse energies of up to 2.6mJ. It has been shown that for the devices under study the emitter size increases only marginally even when operated at 500A peak current and 10µs pulse duration. The slow axis divergence on the other hand increases steadily and near linearly with increasing operating current. This means that the BPP of the diode increases with higher operating current, even when operated with short pulse durations.

It has been concluded that diode laser bars can be operated at significantly higher peak current than the rated CW maximum current, as long as the pulse duration is kept adequately short. The data is consistent with the 'square root law'.

A brief design study for fiber coupled modules has been conducted based on the results. Achievable peak power for fiber cores of 400µm and 200µm (NA 0.22) have been presented.

While the increase in slow axis divergence reduces the number of bars that can be coupled into a fiber compared to CW mode of operation, higher peak powers can be achieved with lower numbers of bars. This leads to cost and size reduced fiber coupled modules for short pulsed applications.

---

[1] Limited by maximum current of driver (500A). COD threshold may be higher.
[2] BPP exceeds beam quality of fiber. Some clipping may occur.

All devices tested here were mounted to standard passively cooled heat sinks (similar to CS types). In order to further reduce the size and weight of fiber coupled modules for short pulse applications, smaller heat sinks can be used if the duty cycle is sufficiently low.

While the data presented here is illustrative, further testing using a more statistically adequate device population needs to be conducted in order to derive lower uncertainty coefficients to validate the applicability of the ‘square root law’. This will allow the calculation of the damage threshold for any given pulse duration for the diode designs tested. It is further recommended to perform life testing of a number of bars at a peak current 20% below the COD threshold to acquire reliability data while maintaining a safety margin between the COD threshold and the operating current.

## REFERENCES


[1] Mattern, T.(2006). QCW-diode stacks with improved efficiency for space applications, *2nd ESA-NASA Working Meeting on Optoelectronics*; Retrieved from https://escies.org/webdocument/showArticle?id=356&groupid=6

[2] Wenzel, H., Crump, P., Pietrzak, A. *et al* (2010). Theoretical and experimental investigations of the limits to the maximum output of laser diodes. *New Journal of Physics*, *12(8)*, 11. Retrieved from doi:10.1088/1367-2630 /12/8/085007.

[3] Olecki, M., Tomm, J. W., Hempel, M. *et al*; “Emission properties of diode laser bars during pulsed high-power operation”, *Proc. SPIE* 8241, High-Power Diode Laser Technology and Applications X, 824107 (February 9, 2012); Retrieved from doi:10.1117/12.905126

[4] Eliseev, P. G. (2012, August 22). Fiftieth anniversary of diode lasers: early history at Lebedev Institute. *Semicond. Sci. Technol*, *27*(9), 7. Retrieved from doi:10.1088/0268-1242/27/9/090204

[5] Kappeler, F., Mettler, K., & Zschauer, K. H. (1982, December/January). Pulsed-power performance and stability of 880 nm GaAIAs/GaAs oxide-stripe lasers. *Solid-State and Electron Devices, IEE Proceedings I*, *129*(6), 256 - 261. Retrieved from doi:10.1049/ip-i-1.1982.0054

[6] Tomm, J. W., Ziegler, M., Hemple, M., & Elsaesser, T. (2011, March 7). Mechanisms and fast kinetics of the catastrophic optical damage (COD) in GaAs-based diode lasers. *Laser & Photonics Reviews*, *5*(3), 422-441. Retrieved from DOI: 10.1002/lpor.201000023

[7] Bachmann, F., Loosen, P., & Poprawe, R. (2007). *High power diode lasers: Technology and applications* (p. 40). New York: Springer.

[8] Wang, Z., Segref, A., Koenning, T., & Pandey, R. “Fiber coupled diode laser beam parameter product calculation and rules for optimized design”. *Proc. SPIE 7918*, High-Power Diode Laser Technology and Applications IX, 791809 (February 21, 2011); Retrieved from doi:10.1117/12.875386.